

Global characteristics of occurrence of an additional layer in the ionosphere observed by COSMIC/FORMOSAT-3

Biqiang Zhao,^{1,2} Weixing Wan,¹ Xinan Yue,³ Libo Liu,¹ Zhipeng Ren,¹ Maosheng He,^{1,4} and Jing Liu^{1,4}

Received 8 October 2010; revised 10 November 2010; accepted 23 November 2010; published 19 January 2011.

[1] Global observations of electron density profile (EDP) from the COSMIC/FORMOSAT-3 satellites were used to investigate, for the first time, the additional stratification of the F2 layer over the equatorial ionosphere on a global scale, which is called F3 layer. The F3 layer in EDP was recognized through the altitude differential profile featured by two maxima existing from 220 km to the peak height of the electron density. There were ~9,400 cases of F3 layer selected out of ~448, 000 occultation events at low and equatorial areas during the period of April 2006–September 2010. Statistical results show that the highest occurrence of F3 layer appears at dip latitude $7\sim 8^\circ/-7\sim -8^\circ$ for Northern/Southern Hemisphere and is more pronounced during summer months at 10:00–14:00 LT. The occurrence also has a clear longitude dependence during boreal summer, with relatively higher occurrence at $-80\sim -100^\circ$, $-20\sim 20^\circ$, $80\sim 120^\circ$ and $-160\sim -170^\circ$ longitudes, that is possibly associated with the wavenumber-3 diurnal tide (DE3). The results support the principle of the F3 layer proposed by Balan et al. (1998), which in turn validate the accuracy of the retrieval of the COSMIC EDP data. **Citation:** Zhao, B., W. Wan, X. Yue, L. Liu, Z. Ren, M. He, and J. Liu (2011), Global characteristics of occurrence of an additional layer in the ionosphere observed by COSMIC/FORMOSAT-3, *Geophys. Res. Lett.*, 38, L02101, doi:10.1029/2010GL045744.

1. Introduction

[2] An additional ionospheric layer, the F3 layer, was discovered 60 years ago by the ground-based ionosonde measurements which shows that the high frequency end of the $h'-f$ ionogram records a ‘spur’ during morning-noon sector [Ratcliffe, 1951]. Balan et al. [1997] renamed this structure from “G-layer” to F3 layer as it is caused by the same chemical composition as the F region. After that, the subject of the F3 layer received extensive investigations concerning its diurnal, seasonal, and long term variations at different sites in the low and equatorial latitudes [e.g., Balan et al., 1998; Batista et al., 2002; Rama Rao et al., 2005; Uemoto et al., 2007; Zhao et al., 2011]. Most studies

are based on the observations of single or several stations distributed at South American, South-East Asian, and Indian areas, unable to give the refined spatial distribution of the F3 layer. Lynn et al. [2000] first presented the latitudinal dependence of the F3 layer occurrence at the equatorial latitudes in South East Asia using the observations from a number of oblique and vertical ionosondes. They found that the region of maximum F2 layer stratification lay between the magnetic equator and the peak of the southern equatorial ionization anomaly (EIA). Another indirect method to estimate the latitude dependence of the F3 layer occurrence was through an investigation of long term ionogram data at an equatorial station Fortaleza in Brazil [Batista et al., 2002], which shows that the F3 layer occurrence decreases with decreasing dip angle. The maximum occurrence appears during 1995–1998 while magnetic dip angle lies in $8.9\sim 10.4^\circ$. Also, the position of the appearance of the F3 layer is investigated through the single station TEC measurements using radio beacon transmissions from LEO satellites [Thampi et al., 2007]. They have found a hump structure in the latitude variation of vertical TEC centered at magnetic latitude $7\sim 8^\circ\text{N}$ at longitude 80°E .

[3] In this study, we investigate the F3 layer structure at low latitude area using the electron density profiles (EDPs) derived from radio occultation (RO) technique of COSMIC/FORMOSAT-3 (a Constellation Observing System for Meteorology, Ionosphere, and Climate mission, here COSMIC for short) [e.g., Lei et al., 2007]. For the first time we have shown the refined latitude as well as longitude variations of the occurrence of the F3 layer feature at a global scale. The observations are discussed in light of the reports available in literature.

2. Data Resources and Method

[4] The COSMIC constellation provides approximately 24h of local time coverage and globally 1000–2500 vertical EDPs (100–800 km) per day. Preliminary validation study of EDPs data was performed by Lei et al. [2007] which shows that the COSMIC derived ionospheric parameters appear to be consistent with other measurements such as the incoherent scatter radars and ionosondes and with model simulations. The raw observations are processed by the COSMIC Data Analysis and Archive Center (CDAAC) and the processed data are now available for the period from day of year (DOY) 111 in 2006 to DOY 269 in 2010, which provides more than 2,770,000 EDPs. During this period, the level of solar activity is at its minimum phase with average F10.7 of 73.7 sfu ($1 \text{ sfu} = 10^{-22} \text{ Wm}^{-2} \text{ Hz}^{-1}$). This interval is a good period for the investigation of F3 layer since the occurrence of F3 layer is higher during

¹Beijing National Observatory of Space Environment, Institute of Geology and Geophysics, Chinese Academy of Sciences, Beijing, China.

²State Key Laboratory of Space Weather, Chinese Academy of Sciences, Beijing, China.

³COSMIC Program Office, University Corporation for Atmospheric Research, Boulder, Colorado, USA.

⁴Graduate University of Chinese Academy of Sciences, Beijing, China.

periods of low solar activity than high solar activity [Balan *et al.*, 1998].

[5] Since F3 layer is primarily a daytime phenomenon at low latitudes during solar minimum, we restrict the data to -30° – 30° dip latitudes during 06:00–18:00 LT, which reduces the number of RO events to ~448, 000 after performing quality control of the dataset. Figure 1 illustrates the distributions of the number of good quality profiles as function of DOY, local time, dip latitude, and longitude. The data is uniformly distributed in DOY and local time. The occultation event number is relatively small at a longitude scale -10° – 120° , and relatively fewer in the equatorial region because of the high inclination orbit of Low Earth Orbit (LEO) satellite [Mousa *et al.*, 2006].

[6] In Figure 2 (bottom right), ionogram recorded at Kwajalein (9.0° N, 167.2° E, dip latitude 3.8° N) at 01:40 UT on June 28 in 2009 provides an F3 layer example. Both O-mode (red) and X-mode (green) echoes show that the trace in the F2 region has been distorted into two parts. At 400–650 km the O-mode frequency sweeps from 4.4–6.1 MHz. It increases fast at the bottom of the F2 layer and slows down near 5.4 MHz, and then it starts to increase fast again forming an additional layer at the high frequency part. The ionospheric EDPs were retrieved by the SAO-explorer software [Reinisch *et al.*, 2004]. The dNe/dh curve was presented on the right panel. It shows double crests and a trough at the bottom ionosphere, which suggests two maximum gradients in the Ne profile. This structure is diagnosed as a sign of a F3 layer. There are two criteria for the selection of COSMIC EDPs. It is known that the accuracy of COSMIC EDPs retrieval depends on several assumptions, where the most significant one is the spherical symmetry of electron density hypothesis. The large horizontal gradients in the ionospheric electron density at low and equatorial areas can produce a false stratification in the EDPs [Lei *et al.*, 2007]. To exclude this situation, we choose a scale for the track of occultation. The up boundary is set to altitude of maximum electron content (H_{max}) and bottom set $H_{max}-150$ km. The latitude and geographic longitude of the tangent point trajectory within the boundary should not exceed 5° and 15° . Under this condition, we select the occultation events whose orientation is either in 0° – 45° (north 90°) or 135° – 180° to avoid the cases oriented in the north-south direction. In addition, we should also consider some tracks of north-south orientation but with small latitude span. A paratactic condition is set that the latitude of the given track should not exceed 2° . This scheme is based on an assumption that F3 layer is relatively a large structure in the low and equatorial regions. Yue *et al.* [2010] pointed out that Abel retrieval under the spherical symmetry assumption has degraded performance in low altitude and at low latitude region. Thus the second criterion is that the altitude bottom boundary of the selected EDP should be larger than 220 km to avoid the contamination of F1 layer and large retrieval errors. Figures 2 (top) and 2 (bottom left) give an occultation event that fits for the above criteria. The tangent point trajectory within the boundary is near the dip equator at West Pacific area. The criteria used for identifying the profiles with F3 layer is through the altitude changing rate of Ne, dNe/dh which shows a similar double peaks as presented in Figure 2 (bottom left). Quality control was also performed on the stratification case. Those cases with more than 2 layers identified in the range of 220 km– H_{max} was discarded. If double peaks in

dNe/dh were due to a step change in a profile, then the situation was eliminated.

3. Results and Discussions

[7] There are a total of ~9400 F3 layer cases that satisfy the above criteria, and it accounts for 2.07% of the total number of profiles, which is much lower than the occurrence at a single ionosonde site. The low percentage of the COSMIC-derived F3 is due to the strict restrictions on the choice of the RO event and F3 identification in order to avoid the large horizontal gradients and retrieval errors in the ionospheric electron density. It should be mentioned that during the early stage of the COSMIC mission, the geometry of the six microsattellites were not fully outspread. Thus some cases were overlapped and counted repeatedly. However, that is a small part of the whole cases. To reduce the effect of the background dataset distribution, we calculate the percentage of the number divided by the original profile amount. Figure 3a displays the local time distribution of the percent occurrences for the F3 layer. It shows that the number of the F3 layer increases quickly after 08:00 LT and reaches the highest level 4.24% at around 10:30 LT and remains at high level until the 12:00 LT and then become gradually decreased until 18:00 LT. This local time dependence of the F3 layer agrees well with the past ionosonde observations [Balan *et al.*, 1998], and is understood as the vertically upward plasma drifts at and above the F2 layer during the morning-noon period is significant due to the combined effect of the upward $E \times B$ drift and the neutral wind lifting.

[8] Figure 3b illustrates the position of the daytime (06:00–18:00 LT) F3 layer occurrence during two periods: DOY 122–242 (May 1st–August 31st) and 305–365, 0–59 (November 1st–February 28th), which represents the summer and transition period for the Northern and Southern Hemisphere respectively when 40.4% and 37.0% of the total F3 layer cases were registered. It can be seen that F3 layer mainly concentrates at low and equatorial areas and appears with dominant occurrence during summer months in both hemispheres. The solid and dashed lines in the map represent the dip equator and dip latitude $\pm 20^{\circ}$. Figure 3c shows magnetic latitude dependence of the F3 layer. Each bar represents the percent number in 1° latitude bin. The highest occurrence value reaches ~18% appearing at around 7° – 8° / -7° – -8° for the Northern/Southern Hemisphere during summer, inside the usual EIA crest regions at $\pm 12^{\circ}$ – 15° . The result has testified the preliminary results of the magnetic latitude dependence of the F3 layer using the ionosonde [e.g., Lynn *et al.*, 2000; Batista *et al.*, 2002]. There were a small portion of the F3 layer cases appearing in the winter hemisphere at low latitudes reaching 3–4%, which accords well with the previous results showing the F3 layer also exists in winter [Balan *et al.*, 1998]. Figure 3b also shows that there are a few cases of the F3 layer are far from the magnetic equator which was possibly considered as the result of the propagation of atmospheric gravity waves (AGWs) often observed in the middle latitudes [Heisler, 1962].

[9] Figures 3d and 3e reveal the longitude distribution of the F3 layer occurrence during the above two periods, which was rarely addressed in the previous studies because of poor coverage of the ground measurements. Each bar represents the percentage number of 10° bin. As shown in Figure 3d,

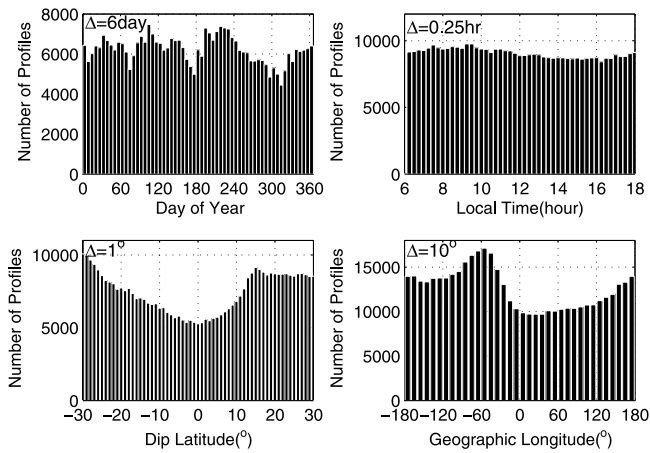


Figure 1. Profile distributions as function of day of year, local time, dip latitude, and longitude within magnetic latitude -30° – 30° .

The count of F3 layer has an obvious longitude variations during boreal summer with higher occurrence at areas of -80° – -100° , -20° – 20° , 80° – 120° and -160° – -170° longitudes. The four-peaked longitudinal structure of F3 layer occurrence resembles the wave-number 4 (WN4) structure which has been detected in a variety of ionospheric parameters. WN4 structure in the ionosphere is considered to be caused by the longitudinal modulation of the F-region ion drifts which is created in turn by the longitudinal modulation of the non-migrating tides, zonal wavenumber-3 diurnal tide (DE3), on the E region dynamo [Immel *et al.*, 2006]. We

have shown the average vertical $E \times B$ plasma drifts (V_{\perp}) near the dip equator in May–August during 09:00–12:00 LT, derived from ROCSAT-1 of an orbit at an altitude 600 km [Fejer *et al.*, 2008]. The longitude variation of V_{\perp} in certain longitudes is in phase of the longitude distribution of F3 layer occurrence which suggests a possible link between the higher occurrence of F3 layer and the DE3 tide in the lower atmosphere. The occurrence of F3 is modulated by the wave structures. It is expected because the occurrence depends mainly on upward $E \times B$ drift and partly on neutral winds and waves. The waves can (1) directly affect the occurrence of F3 through its contribution in changing the F2/F3 heights at locations where geomagnetic and geographic equators do not coincide and also at locations of large field inclination, and (2) indirectly affect the occurrence of F3 by changing the F2/F3 heights by the electric field arising through E region–F region coupling. In the upper thermosphere, the DE3 tide has been found in thermospheric zonal winds based on in situ accelerometer measurements on the Challenging Minisatellite Payload (CHAMP) [Lühr *et al.*, 2007]. They have shown that the longitudinal modulation of the thermospheric zonal wind may not be caused by the wave-4 pattern of the EIA through the ion drag. Because of the polar orbit of the CHAMP satellite, longitudinal variations in the meridional winds cannot be obtained at the satellite altitudes. Whether the thermospheric meridional winds have DE3 component and make a contribution to the ionospheric wave-4 pattern structure remains open and yet to be resolved.

[10] In comparison, Figure 3e shows no WN4 structure during December–February period. The absence of WN4 structure can also be found in the TEC at EIA region and

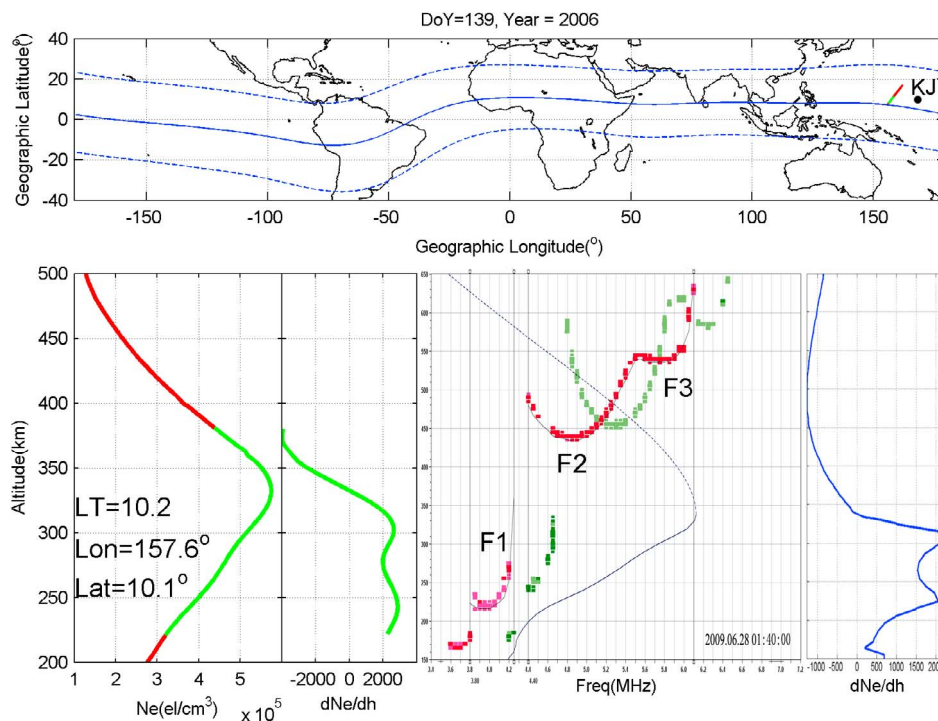


Figure 2. An occultation event characterized by F3 layer structure and an F3 layer recorded at Kwajalein at 01:40 UT on June 28, 2009. (top) The tangent point trajectory and position of Kwajalein. (bottom) From left to right, gives EDP, altitude differential of EDP, Ne and dNe/dh profile derived from the SAO-software. The green line represents the value within $H_{\max} -150$ km to $H_{\max} +50$ km.

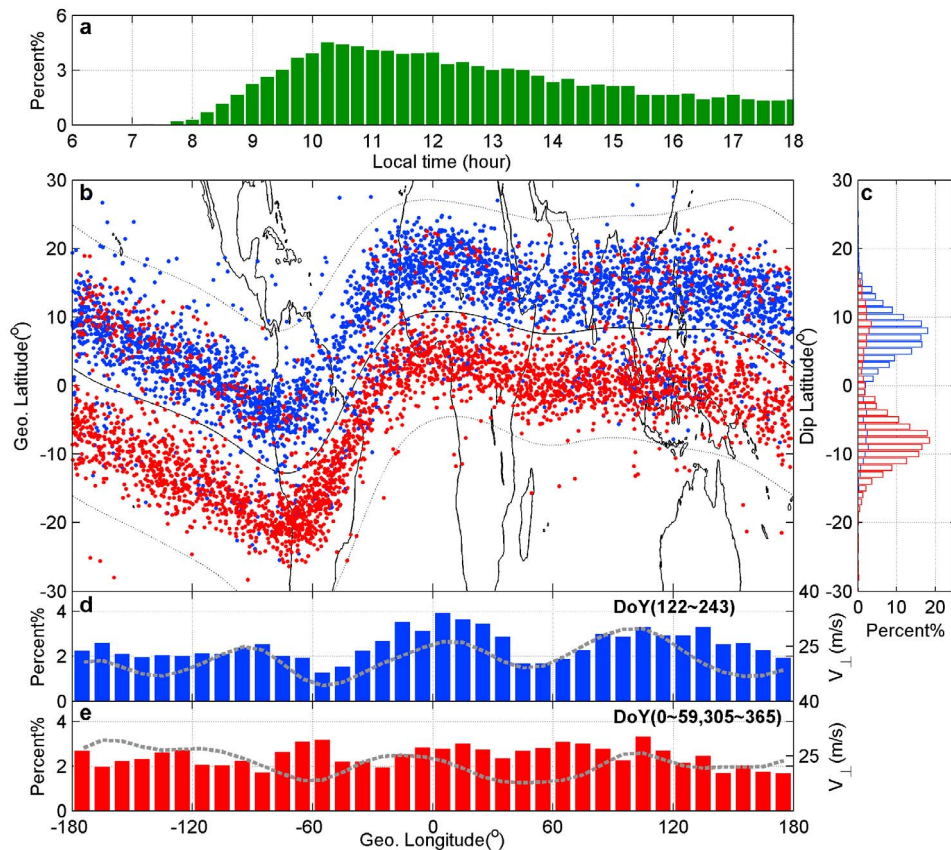


Figure 3. F3 layer occurrence as a function of (a) local time, (b) geographic position of the F3 layer during 06:00–18:00 LT in boreal summer (blue) and winter (red), (c) dip latitude, (d) geographic longitude during boreal summer, and (e) winter. ROCSAT-1 derived equatorial vertical drift V_{\perp} (gray) were superimposed on Figures 3d and 3e.

equatorial vertical $E \times B$ plasma drifts V_{\perp} and other ionospheric parameters [e.g., Ren *et al.*, 2009]. This seasonal variation could be most probably caused by the intra-annual variations of DE3 in terms of latitudinally symmetric versus antisymmetric modes, where detailed description was given by Ren *et al.* [2009]. The average vertical $E \times B$ plasma drifts (V_{\perp}) near the dip equator in Nov–February during 09:00–12:00 LT was superimposed on the panel. One can note that there is large difference between the drift pattern and F3 layer distribution. The drift pattern shows large amplitude at -180° – 90° while the occurrence of F3 layer was not that high. Perhaps the zonal wind may provide a clue in understanding the discrepancy. The daytime westward zonal wind could retard the equatorward wind along the magnetic meridian blowing from Southern Hemisphere at the longitudes of largely positive magnetic declination (-190° – 60°). There is evidence that the zonal wind can effectively affect the longitude distribution of topside plasma density at equatorial area. The topside plasma density N_i of 17:45 LT during Nov–February, measured by DMSP F13 satellite, is quite low at -190° – 60° comparing with the other longitudes [Ren *et al.*, 2008]. However, there is still a discrepancy that cannot be associated with the upward drift such as the higher occurrence of F3 layer at -60° and 60° . The formation of the F3 layer depends on the combined effect of electric field and neutral wind, and even the neutral density. Raghavarao and Sivaraman [1974] proposed that neutral density enhancements along the ionization anomaly field line

can inhibit the downward ambipolar diffusion of the plasma and result in the equatorial topside ledge. Recently, wave-4 pattern of the equatorial mass density anomaly (EMA) near equinox in 2002 was revealed by Liu *et al.* [2009], which shows a different phase from that of EIA in certain regions. We are not able to explain all the longitude features of F3 layer because of the absence of actual longitude distribution of electric field and neutral wind and neutral density during the year 2006–2010. However, our findings show that during boreal summer, the factors seem favorable for the formation of WN4 pattern of F3 layer. In future, more data will be used and collaborative work with the C/NOFs Neutral Wind Meter (NWM) data might be expected to explain the longitude variation of the F3 layer.

4. Summary

[11] This paper presents a statistical work to infer the F3 layer structure directly from COSMIC RO data. Basic morphology and properties of F3 layer occurrence during 2006–2010 are investigated. The major findings presented herein are summarized as follows: it is the first time the stratification structure of the F2 region is investigated by the COSMIC EDPs. The location of the F3 layer occurrence on a global scale are presented, which clearly shows the existence of the F2 stratification as a regular phenomenon at all the longitudes and have delineated its rapid variation with latitude in a narrow zone of occurrence. Meanwhile, the

longitude difference of the F3 layer, which shows WN4 pattern in boreal summer, provides an indirect clue that the DE3 of lower atmosphere changes not only a single parameter in the ionosphere but also the whole altitude structure of the F region. These results indicate that the RO soundings are of sufficient high accuracy to differentiate the variation of very local and subtle structure, although more RO events are needed to derive the refined structure of the ionospheric profiles at the low and equatorial latitudes.

[12] **Acknowledgments.** This research was supported by National Natural Science Foundation of China (40804041) and National Important Basic Research Project of China (2011CB811405), and also by Open Research Program of State Key Laboratory of Space Weather, Chinese Academy of Sciences.

References

- Balan, N., G. J. Bailey, M. A. Abdu, K. I. Oyama, P. G. Richards, J. Macdougall, and I. S. Batista (1997), Equatorial plasma fountain and its effects over three locations: Evidence for an additional layer, the F3 layer, *J. Geophys. Res.*, *102*, 2047–2056, doi:10.1029/95JA02639.
- Balan, N., I. S. Batista, M. A. Abdu, J. Macdougall, and G. J. Bailey (1998), Physical mechanism and statistics of occurrence of an additional layer in the equatorial ionosphere, *J. Geophys. Res.*, *103*, 29,169–29,181, doi:10.1029/98JA02823.
- Batista, I. S., M. A. Abdu, J. McDougall, and J. R. Souza (2002), Long term trends in the frequency of occurrence of the F3 layer over Fortaleza, *J. Atmos. Sol. Terr. Phys.*, *64*, 1409, doi:10.1016/S1364-6826(02)00104-9.
- Fejer, B. G., J. W. Jensen, and S.-Y. Su (2008), Quiet time equatorial F region vertical plasma drift model derived from ROCSAT-1 observations, *J. Geophys. Res.*, *113*, A05304, doi:10.1029/2007JA012801.
- Heisler, L. H. (1962), The anomalous ionospheric stratification F1.5, *J. Atmos. Sol. Terr. Phys.*, *24*, 483–489, doi:10.1016/0021-9169(62)90212-X.
- Immel, T. J., E. Sagawa, S. L. England, S. B. Henderson, M. E. Hagan, S. B. Mende, H. U. Frey, C. M. Swenson, and L. J. Paxton (2006), Control of equatorial ionospheric morphology by atmospheric tides, *Geophys. Res. Lett.*, *33*, L15108, doi:10.1029/2006GL026161.
- Lei, J., et al. (2007), Comparison of COSMIC ionospheric measurements with ground-based observations and model predictions: Preliminary results, *J. Geophys. Res.*, *112*, A07308, doi:10.1029/2006JA012240.
- Liu, H., M. Yamamoto, and H. Lühr (2009), Wave-4 pattern of the equatorial mass density anomaly: A thermospheric signature of tropical deep convection, *Geophys. Res. Lett.*, *36*, L18104, doi:10.1029/2009GL039865.
- Lühr, H., K. Häusler, and C. Stolle (2007), Longitudinal variation of F region electron density and thermospheric zonal wind caused by atmospheric tides, *Geophys. Res. Lett.*, *34*, L16102, doi:10.1029/2007GL030639.
- Lynn, K. J. W., T. J. Harris, and M. Sjarifudin (2000), Stratification of the F2 layer observed over Southeast Asia, *J. Geophys. Res.*, *105*, 27,147–27,156, doi:10.1029/2000JA900056.
- Mousa, A., Y. Aoyama, and T. Tsuda (2006), A simulation analysis to optimize orbits for a tropical GPS radio occultation mission, *Earth Planets Space*, *58*, 919–925.
- Raghavarao, R., and M. R. Sivaraman (1974), Ionization ledges in the equatorial ionosphere, *Nature*, *249*, 331–332, doi:10.1038/249331a0.
- Rama Rao, P. V. S., K. Niranjana, D. S. V. V. D. Prasad, P. S. Brahmanandam, and S. Gopikrishna (2005), Features of additional stratification in ionospheric F2 layer observed for half a solar cycle over Indian low latitudes, *J. Geophys. Res.*, *110*, A04307, doi:10.1029/2004JA010646.
- Ratcliffe, J. A. (1951), Some regularities in the F2 region of the ionosphere, *J. Geophys. Res.*, *56*, 487–507, doi:10.1029/JZ056i004p00487.
- Reinisch, B. W., I. A. Galkin, G. Khmyrov, A. Kozlov, and D. F. Kitrosser (2004), Automated collection and dissemination of ionospheric data from the digisonde network, *Adv. Radio Sci.*, *2*, 241–247, doi:10.5194/ars-2-241-2004.
- Ren, Z., W. Wan, L. Liu, B. Zhao, Y. Wei, X. Yue, and R. A. Heelis (2008), Longitudinal variations of electron temperature and total ion density in the sunset equatorial topside ionosphere, *Geophys. Res. Lett.*, *35*, L05108, doi:10.1029/2007GL032998.
- Ren, Z., W. Wan, L. Liu, and J. Xiong (2009), Intra-annual variation of wave number 4 structure of vertical $E \times B$ drifts in the equatorial ionosphere seen from ROCSAT-1, *J. Geophys. Res.*, *114*, A05308, doi:10.1029/2009JA014060.
- Thampi, S. V., N. Balan, S. Ravindran, T. K. Pant, C. V. Devasia, P. Sreelatha, R. Sridharan, and G. J. Bailey (2007), An additional layer in the low-latitude ionosphere in Indian longitudes: Total electron content observations and modeling, *J. Geophys. Res.*, *112*, A06301, doi:10.1029/2006JA011974.
- Uemoto, J., T. Ono, T. Maruyama, S. Saito, M. Iizima, and A. Kumamoto (2007), Magnetic conjugate observation of the F3 layer using the SEALION ionosonde network, *Geophys. Res. Lett.*, *34*, L02110, doi:10.1029/2006GL028783.
- Yue, X., W. S. Schreiner, J. Lei, S. V. Sokolovskiy, C. Rocken, D. C. Hunt, and Y.-H. Kuo (2010), Error analysis of Abel retrieved electron density profiles from radio occultation measurements, *Ann. Geophys.*, *28*, 217–222, doi:10.5194/angeo-28-217-2010.
- Zhao, B., W. Wan, B. Reinisch, X. Yue, H. Le, J. Liu, and B. Xiong (2011), Features of the F3 layer in the low-latitude ionosphere at sunset, *J. Geophys. Res.*, doi:10.1029/2010JA016111, in press.

M. He, J. Liu, L. Liu, Z. Ren, W. Wan, and B. Zhao, Beijing National Observatory of Space Environment, Institute of Geology and Geophysics, Chinese Academy of Sciences, Beijing 10029, China. (zbqjz@mail.iggcas.ac.cn)

X. Yue, COSMIC Program Office, University Corporation for Atmospheric Research, PO Box 3000, Boulder, CO 80307, USA.